Journal of Alloys and Compounds 505 (2010) 549–554

Contents lists available at ScienceDirect

Journal of Alloys and Compounds

journal homepage: www.elsevier.com/locate/jallcom

Monitoring of hydrogen absorption/desorption into pressed cobalt powder using resistometry

M. Spasojević[a], N. Krstajić[b], L. Ribić Zelenović[a,*], A. Maričić[a]

[a] Joint Laboratory for Advanced Materials of the Serbian Academy of Science and Arts, Section for Amorphous Systems, Svetog Save 65, 32000 Čačak, Serbia
[b] University of Belgrade, Faculty of Technology and Metallurgy, Karnegijeva 4, 11000 Belgrade, Serbia

ARTICLE INFO

Article history:
Received 17 July 2009
Received in revised form 10 June 2010
Accepted 11 June 2010
Available online 23 June 2010

Keywords:
Powder metallurgy
Hydrogen absorbing materials

ABSTRACT

The kinetics of hydrogen absorption/desorption into pressed cobalt powder samples was monitored using resistometry. The samples were prepared by pressing Co powder at 100 MPa and $t = 25\,^{\circ}C$. The equivalent diameter of the species varied from 5 to 200 μm. The study showed that hydrogen absorption leads to an increase in the electrical resistivity of the pressed samples. During diffusion into the crystal lattice, the absorbed hydrogen atoms simultaneously trap an electron from the conduction band of the metal and form H^- ions, consequently inducing an increase in the electrical resistivity of the pressed sample. On the basis of the change in resistivity, a mechanism of hydrogen absorption has been proposed. During the initial period of absorption, the hydrogen absorption reaction is limited by the dissociative adsorption of hydrogen over a short period of time, following which the diffusion of H^- ions into the bulk of the pressed Co powder is identified as the rate-determining step. The hydrogen desorption rate in an argon atmosphere is limited by $H_{2,ad}$ formation; recombination of adsorbed hydrogen atoms, H_{ad}, or by the diffusion of H^- ions from the crystal lattice over a prolonged period of time.

1. Introduction

Metal hydrides are formed by reacting hydrogen with metals or alloys. Most metal hydrides can attain very high densities of hydrogen that can be as high as liquid hydrogen. Large amounts of hydrogen are absorbed in small volumes by these metals at room temperature and under a pressure close to atmospheric pressure. These metals and alloys have been used in many fields, such as heat pumps, thermal storage systems, as catalysts, fuel cells, nickel–metal hydride rechargeable batteries, etc. An alloy can be successfully employed for hydrogen storage if it exhibits not only a large hydrogen capacity, but also high hydrogen absorption/desorption rate [1–5]. For these reasons, a large number of experimental and numerical studies have been conducted to understand and model the mechanisms controlling the hydrogen absorption and desorption kinetics [2–11]. Many inexpensive metals absorb large amounts of hydrogen (magnesium and magnesium-rich alloys); however, they show slow hydrogenation/dehydrogenation kinetics. Therefore, various studies have been undertaken to explore the possibility of enhancing the rate of hydrogenation and dehydrogenation. The influences of the additions, the preparation methods, and the element substitution on the hydriding reaction kinetics mechanisms of magnesium-rich alloy-based composites have been systematically investigated [12–22].

The electrochemical properties of negative electrodes (hydrogen storage alloys) used in secondary nickel–metal hydride batteries, are dependent upon the preparation method employed, chemical composition and microstructure [23–25]. The mechanical properties and corrosion rates of a number of metals and alloys that find wide applications under aggressive corrosion conditions (e.g. titanium and its alloys) are governed by hydrogen content [26–29]. Corrosion rate and degradation rate of mechanical properties (strength and toughness) are observed to increase with increasing hydrogen content [30–37]. Studies on the hydrogen absorption/desorption kinetics of the above alloys have resulted in diverse experimental data and varied interpretations of the said processes [30–37].

Resistometry has been used for *in situ* monitoring of steel corrosion [38,39], passive films on iron [40,41] and anodic dissolution and pitting of iron [42]. In this technique, the change in electrical resistivity is associated with shrinking of electrodes due to corrosion loss or to change in electrical properties of materials due to composition changes. Resistometry is also used to evaluate the hydrogen content in Pd as resistivity is dependent on the atomic ratio, H/Pd. Conclusion on the electrical resistance of PdH_x versus composition x and correlated physical phenomena have been done [43–49]. The resistivity of Ti has also been reported to

* Corresponding author. Tel.: +381 32 303 408; fax: +381 32 303 401.
E-mail addresses: lenka@tfc.kg.ac.rs (M. Spasojević), gaja@tfc.bg.ac.rs (N. Krstajić), lenka@tfc.kg.ac.rs (L.R. Zelenović), marec@tfc.kg.ac.rs (A. Maričić).

0925-8388/$ – see front matter © 2010 Elsevier B.V. All rights reserved.
doi:10.1016/j.jallcom.2010.06.070

change with hydrogen content [50–53]. The electrical conductivity of a Ti hydride is considerably lower than that of a Ti metal. The electrical resistivity of many alloys [FeTi, NiTi, FeTiMn, LaNi, $LaCo_5$, $ZrMn_{2-x}Fe_x$, RM_3 (R = rare earth metals, M = metals), RTM*n* (TM = transition metal; *n* = 1.2 or 5), $MmTM_3$ (Mm = Mischmetal, a natural mixture of light rare earth metals)] increases with increasing absorbed hydrogen content [54–65]. The increase in resistivity is associated with the penetration of adsorbed H atoms into the interstitial sites of the alloy crystal lattice and the electron trapping from the conduction band, simultaneously inducing an increase in lattice parameters. The lattice expansion and decrease in the number of conduction electrons lead to a decrease in electrical resistivity [54–65].

Azhazha et al. [66] have reported that absorbed hydrogen causes an increase in the electrical resistivity of the amorphous alloy $Ti_{66}Ni_{20}Cu_{10}Si_4$. The origin of the excess resistivity may be attributed to electron scattering on the deformed phonon spectrum and the interference of the latter scattering with inelastic scattering of electrons on hydrogen.

The objective of the present study was, therefore, to examine the applicability of resistometry as an *in situ* technique for monitoring hydrogen absorption into pressed Co powder. Resistivity was monitored during hydrogen absorption into a pressed Co powder having a small cross-sectional area. The resistivity data were used to analyze growth of the hydride layer.

2. Experimental

Cobalt powder (5–200 μm) was pressed at $p = 100$ MPa and $t = 25\,^{\circ}C$. The pressed samples were in the shape of a parallelepiped having the following dimensions: 40 mm × 1 mm × 0.4 mm. The kinetics of hydrogen absorption/desorption was determined through the change in the electrical resistivity of the pressed samples. Resistivities were measured by the four-point method using a high-sensitivity 10^{-5} V ISKRA voltmeter. The samples were placed in a furnace in flowing hydrogen, argon or their mixture at a constant total pressure of 101.3 kPa.

The change in electrical resistivity was measured as a function of time at constant temperatures of 160, 180, 200, 230 and 260 °C and at hydrogen partial pressures of 101, 81, 61, 40.3 and 20.2 kPa.

The pressure drop of hydrogen, Δp, measured in a closed chamber containing the hydrogen absorbing sample, was used to determine the dependence of the electrical resistivity of the pressed cobalt powder sample on the amount of hydrogen absorbed.

The pressed sample having a mass of *m* was placed in the chamber filled with hydrogen, its volume being *V*, at a pressure of $p = 101.3$ kPa and temperature of $t = 200\,^{\circ}C$. The dependence of the electrical resistivity of the sample on the hydrogen pressure drop in the chamber was measured. The amount of absorbed hydrogen, $\Delta n(H_2)$, was determined using the following equation:

$$\Delta n_{H_2} = \Delta p_{H_2} \frac{V}{RT}$$

where *R*: the universal gas constant; *T*: absolute temperature.

The crystal structure and grain size of Co-samples were determined by X-ray diffraction (XRD) analysis using a Philips MRD diffractometer with Cu-K_α radiation.

3. Experimental results

Fig. 1 shows the isothermal dependence of the change in the electrical resistivity ($\Delta\rho$) of the pressed Co sample on hydrogen partial pressure at different temperatures after 500 s of hydrogen absorption. The figure indicates that the increase in resistivity is proportional to the partial pressure of hydrogen, or in other words, the change in the electrical resistivity of the pressed Co powder sample is proportional to the concentration of absorbed hydrogen.

Fig. 2 shows the dependence of the reciprocal value of electrical resistivity, $1/\rho$, on the amount of hydrogen absorbed per cobalt mole, $2\Delta n_{H_2}/n_{Co}$.

Fig. 3 illustrates the dependence of the change in electrical resistivity as a function of time during hydrogen absorption at $p_{H_2} = 101.3$ kPa at various temperatures. The experimental data show that hydrogen absorption leads to an increase in the electrical resistivity of the pressed cobalt powder.

Following hydrogen absorption at a constant temperature, the kinetics of hydrogen desorption was investigated by replacing the hydrogen atmosphere with argon in the furnace. The change in the electrical resistivity of the pressed Co powder during hydrogen desorption is shown in Fig. 4.

The phase structure of the pressed Co powder was determined before and after hydrogenation using XRD analysis. In both cases, the obtained XRD diagrams showed

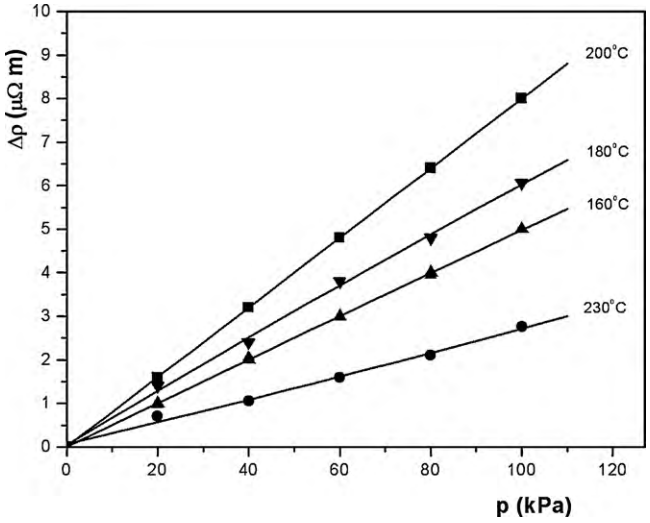

Fig. 1. Variation of electrical resistivity ($\Delta\rho = \rho - \rho_0$) as dependent on hydrogen partial pressure (p_{H_2}) in pressed Co powder after 500 s of hydrogen absorption at different temperatures.

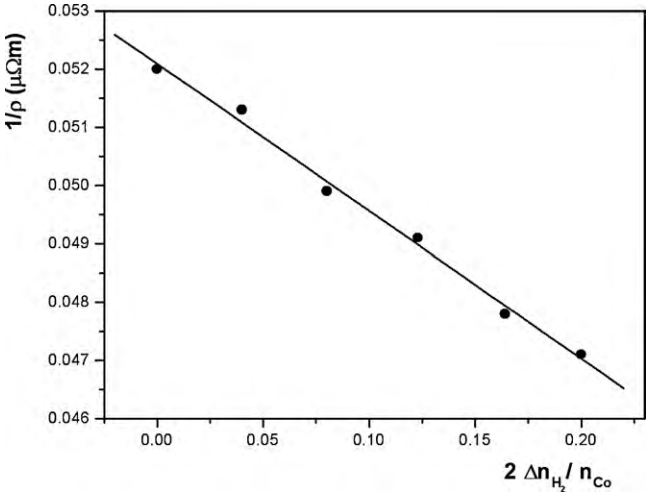

Fig. 2. Dependence of $1/\rho$ on $2\Delta n(H_2)/n(Co)$ at $t = 200\,^{\circ}C$: $\Delta n(H_2)$: the amount of absorbed hydrogen; $n(Co)$: amount of Co.

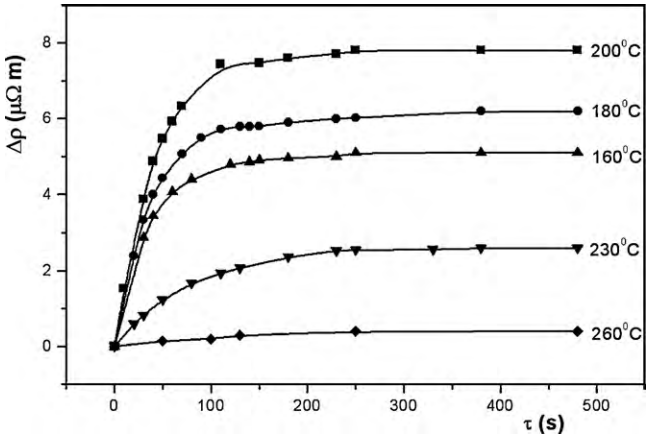

Fig. 3. Time variation of electrical resistivity ($\Delta\rho = \rho - \rho_0$) during hydrogen absorption into pressed Co powder at $p_{H_2} = 101.3$ kPa at various temperatures.

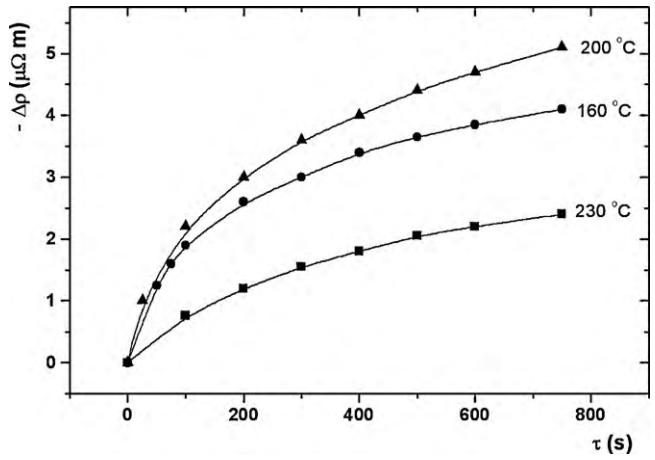

Fig. 4. Dependence of the change in electrical resistivity ($\Delta\rho = \rho - \rho_0'$) during hydrogen desorption, τ, from pressed Co powder at various constant temperatures ($\rho = \rho_0'$ for $\tau = 0$).

the presence of only the hcp-phase. The lattice parameter values were identical prior to and upon heating and hydrogenation (a = 2.5007Å, c = 4.0564 Å).

4. Discussion

XRD measurements showed that the freshly pressed cobalt powder samples and the samples heated to temperatures of 160, 180, 200, 230 and 260 °C in hydrogen contain only the hcp-phase. The calculated values of the lattice parameters a and c were identical for all samples, suggesting that heating to 260 °C and hydrogen absorption did not change the unit cell volume of the crystal lattice. Other authors [67–73] have also shown that the Co–H system in H_2 atmosphere at pressures lower than 5 GPa and temperatures below 365 °C contain only the hcp-phase of Co–H. Hydrogen absorption at temperatures lower than 300 °C was found not to induce lattice contraction. Moreover, superabundant vacancy formation does not take place under the said conditions, and the absorbed H atoms were observed to occupy interstitial sites [67].

The experimental data (Figs. 2 and 3) show that hydrogen absorption leads to an increase in the electrical resistivity of the pressed cobalt powder. The increase in resistivity is probably due to a decrease in the number of free electrons in the conduction band. The decrease occurs as a result of free electron trapping by absorbed hydrogen atoms. The formed H^- ions are located in interstitial sites. H^- ions also exist in the crystal structure of alkali and earth alkali metal hydrides. The assumption that H^- ions exist in the Co–H phase can be confirmed by determining the mechanism and kinetic expression for hydrogen absorption and desorption in the Co-H phase and identifying whether the experimentally obtained values of the time-dependent change in electrical resistivity fit the kinetic expression well.

The shape of the $\Delta\rho = f(\tau)$ relationship indicates that hydrogen absorption is a very complex reaction. Analyzing the time variation of electrical resistivity during hydrogen absorption/desorption at various temperatures, the following hydrogen absorption mechanism can be proposed:

$$H_2 \underset{k_{-1}}{\overset{k_1}{\rightleftarrows}} H_{2,ad} \quad (1)$$

$$H_{2,ad} \xrightarrow{k_2} 2H_{ad} \quad (2)$$

$$2H_{ad} + 2e^- \underset{k_{-3}}{\overset{k_3}{\rightleftarrows}} 2H^- \quad (3)$$

where k_1, k_2 and k_3 are the rate constants for the direct chemical reactions (1), (2) and (3), respectively, and k_{-1}, k_{-2} and k_{-3} the rate constants for the respective reactions in the backward direction.

The overall reaction for the initial stage of absorption is controlled by dissociation of adsorbed hydrogen molecules, while that for prolonged absorption is governed by the diffusion of H^- ions into the crystal lattice of Co.

When the overall reaction is controlled by step 2, the reaction rate will be:

$$-\frac{dC_{H_{2,ad}}}{d\tau} = k_2 C_{H_{2,ad}} \quad (4)$$

Or, by integrating Eq. (4), the time dependence of the concentration of adsorbed hydrogen is obtained:

$$\ln C_{H_{2,ad}} = k_2\tau + \ln C^0_{H_{2,ad}} \quad (5)$$

where $C^0_{H_{2,ad}}$ is the concentration of the adsorbed hydrogen molecule for $\tau = 0$ and $C_{H^-} = 0$.

The surface concentration of adsorbed hydrogen can be expressed in terms of the surface coverage, $\Theta_{H_{2,ad}}$:

$$C_{H_{2,ad}} = k_a \Theta_{H_{2,ad}} \quad (6)$$

In reaction (3) if penetration of H atoms from the surface into the crystal lattice with simultaneous trapping of an electron from the conduction band is much faster than reaction (2), then reaction (3) is assumed to be in quasi-equilibrium, meaning that:

$v_3 = v_{-3}$ or :

$$k_3 \Theta_{H_{ad}} = k_{-3} C_{H^-} \quad (7)$$

and

$$\Theta_{H_{ad}} = \frac{k_{-3}}{k_3} C_{H^-} \quad (8)$$

where: v_3 and v_{-3} stand for rates of chemical reaction (3) in the direct and backward directions, respectively.

Electrical conductivity, χ, is proportional to the concentration of free electrons, n_e:

$$\frac{1}{\rho} = \chi = k_4(n_e^0 - C_{H^-}) \quad (9)$$

where n_e^0 is the concentration of free electrons for $C_{H^-} = 0$. By combining Eqs. (8) and (9), the ($\Theta_{H_{ad}} - (1/\rho)$ relationship is obtained.

Using the following relationship:

$$\Theta_{H_{2,ad}} = 1 - \Theta_{H,ad}. \quad (10)$$

If reaction (2) is the rate-determining step, by combining Eqs. (10), (9) and (6), it is possible to derive the time dependence of the electrical resistivity for hydrogen absorption for the proposed mechanism:

$$\ln\left(K + \frac{1}{\rho}\right) = k_2\tau + \ln\left(K + \frac{1}{\rho^0}\right) \quad (11)$$

where K is the constant including appropriate above mentioned rate constants: $K = k_4((k_3/k_3) - n_e^0)$. The values of the constant K were calculated as follows. Eq. (11) was assumed to be valid for initial hydrogen absorption. The experimentally determined values for ρ_1,τ_1 and ρ_2,τ_2 and Eq. (11) were used to calculate K and k_2 values. This step was repeated for different values experimentally determined for ρ_x,τ_x and ρ_y,τ_y. The obtained K and k_2 values were used to calculate their mean values. The $\ln(K+(1/\rho))$ values were calculated from the mean K value and the experimentally determined ρ values. Based on the calculated values, $-\ln(K+(1/\rho))$ was plotted as a function of τ (Fig. 5.). The obtained linear dependence

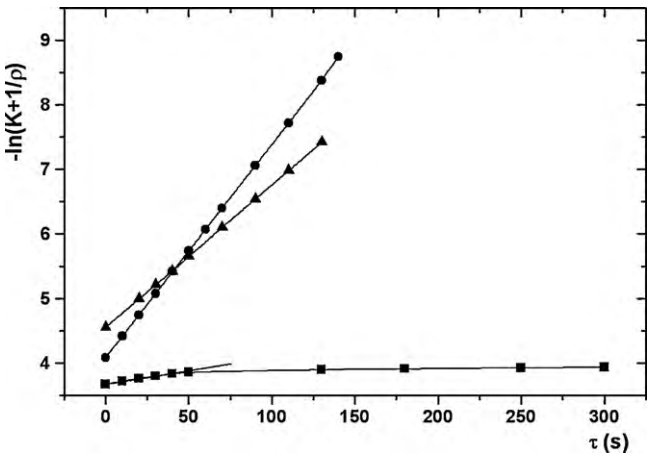

Fig. 5. $-\ln(K+(1/\rho))$ as a function of time, τ, at constant temperatures of: (■) 230 °C; (●) 200 °C; (▲) 180 °C, during hydrogen absorption into pressed Co powder.

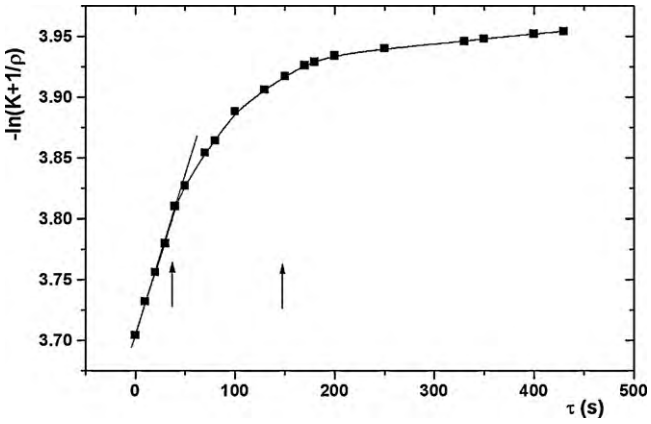

Fig. 6. $-\ln(K+(1/\rho))$ as a function of time, τ, for hydrogen absorption into Co powder at 230 °C and $p_{H_2} = 101.2$ kPa.

of $-\ln(K+(1/\rho))$ on τ confirms the validity of both Eq. (11) for initial hydrogen absorption and the calculated mean values of K and k_2. The K and k_2 values were determined at 160, 180, 200 and 230 °C.

Fig. 5 illustrates a linear relationship between $-\ln(K+(1/\rho))$ and τ during the initial period of hydrogen absorption, showing evidence of the hydrogen absorption reaction being limited by the dissociation of adsorbed hydrogen molecules. This linear dependence occurs only for the absorption period of 40 s at 230 °C (Fig. 6).

The dependence of the reciprocal value of resistivity, $1/\rho$, on $\tau^{1/2}$ for hydrogen absorption into Co powder at 230 °C and $p_{H_2} = 101.3$ kPa is shown in Fig. 7. The curve can be divided into three parts. The first part of the curve is determined by the slow dissociation of adsorbed hydrogen molecules. The second part of the curve ($40\,s < \tau < 150$ s) is determined by the mixed control of hydrogen absorption, while the linear third part is dependent on the slow diffusion of H^- ions into the Co crystal lattice.

The temperature-induced increase in the rate of elemental reaction step 2 is much higher than that of the diffusion of H^- ions into the crystal lattice of Co leading to shortening of the first linear part of the $-\ln(K+(1/\rho)) - \tau$ curve.

The obtained linear dependence of $-\ln(K+(1/\rho))$ on τ and $1/\rho$ on $\tau^{1/2}$ during the initial and third time intervals, respectively, confirms the validity of the proposed mechanism of hydrogen absorption and the existence of H^- ions in the Co–H phase.

The kinetics of hydrogen desorption was determined based on the experimentally obtained diagrams showing the dependence of the change in the electrical resistivity of the pressed cobalt powder on the duration of hydrogen desorption (Fig. 4). A comparison of the results presented in Figs. 3 and 4 suggests that the desorption reaction is slower than absorption.

In the proposed mechanism, the recombination of adsorbed hydrogen atoms is the rate-determining step (*reaction (2) in backward direction*).

The desorption rate can be expressed using the following equation:

$$\frac{-2\mathrm{d}\Theta_{H,ad}}{\mathrm{d}\tau} = k_{-2}\Theta_{H,ad}^2 \tag{12}$$

Integrating Eq. (12) gives:

$$\frac{1}{\Theta_{H,ad}} = \frac{1}{\Theta_{H,ad}^o} + \frac{k_{-2}}{2}\tau \tag{13}$$

Assuming that reaction (3) is in quasi-equilibrium, then $v_3 = v_{-3}$, or:

$$k_3\Theta_{H,ad} = k_{-3}C_{H^-} \tag{14}$$

Combining Eqs. (13) and (14) yields the following expression:

$$\frac{k_3}{k_{-3}C_{H^-}} = \frac{k_3}{k_{-3}C_{H^-}^{0/}} + \frac{k_{-2}}{2}\tau \tag{15}$$

where $C_{H^-}^{0/}$ is the concentration of C_{H^-} for $\tau = 0$.

The following equation can be derived from Eq. (9):

$$\Delta\frac{1}{\rho} = \frac{1}{\rho_p} - \frac{1}{\rho} = k_4C_{H^-} \quad \text{and} \quad \Delta\frac{1}{\rho_o} = \frac{1}{\rho_p} - \frac{1}{\rho_0'} = k_4C_{H^-}^{0/} \tag{16}$$

where ρ_p is the electrical resistivity of non-hydrogenated pressed samples and ρ_0' is the electrical resistivity for $\tau = 0$.

Using Eqs. (15) and (16), the following time dependence of $\Delta(1/\rho)$ for hydrogen desorption is derived:

$$\frac{1}{\Delta(1/\rho)} = \frac{1}{\Delta(1/\rho_o)} + a\tau \tag{17}$$

where: $a = k_2k_{-3}/2k_4k_3$.

In the initial stage of hydrogen desorption, a linear dependence between $(\Delta(1/\rho))^{-1}$ and time occurs at all temperatures (Fig. 8). The linear relationship proves the assumption that the overall rate of hydrogen desorption at the beginning of desorption is controlled by reaction step 2 in the backward direction.

Fig. 9 shows the dependence of the reciprocal value of resistivity on $\tau^{1/2}$. $1/\rho$ depends linearly on $\tau^{1/2}$ during prolonged desorption, indicating that the reaction is controlled by the diffusion of H^- ions.

The experimental results shown in Figs. 3–9 undoubtedly indicate that the overall reaction is kinetically controlled (*reaction*

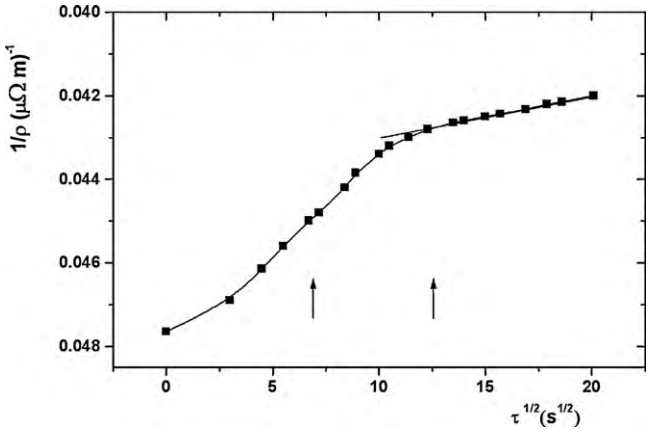

Fig. 7. Reciprocal value of the resistivity of pressed Co powder, $1/\rho$, as a function of $\tau^{1/2}$, for hydrogen absorption at 230 °C and $p_{H_2} = 101.3$ kPa.

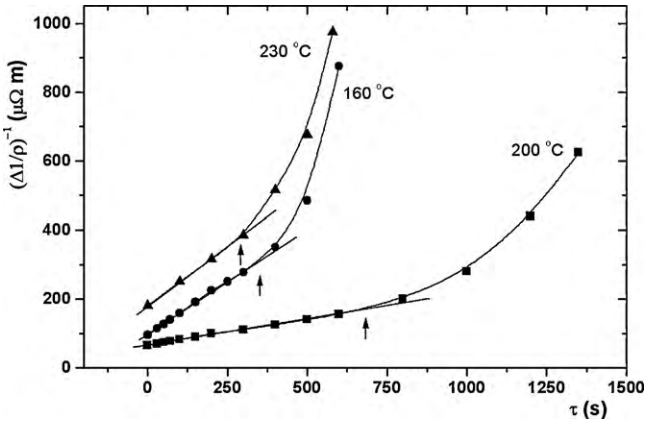

Fig. 8. $(\Delta 1/\rho)^{-1}$ as a function of time, τ, for hydrogen desorption from pressed Co powder at various temperatures: (●) 160 °C; (▲) 200 °C; (■) 230 °C.

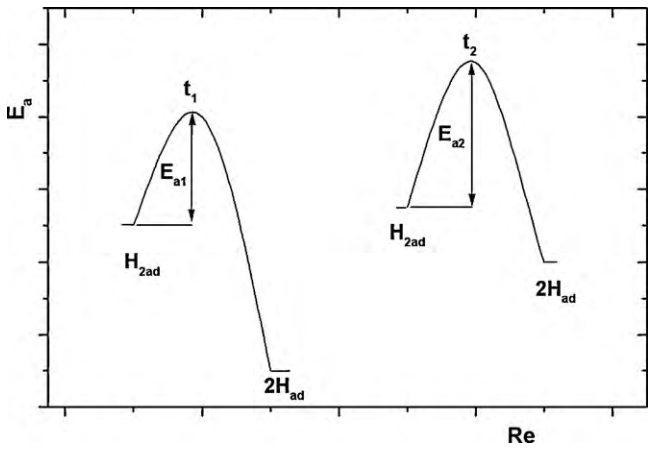

Fig. 10. Activation energy of reaction (2).

(2)) in the initial stage of hydrogen absorption/desorption at the pressed Co powder. For prolonged absorption, the reaction is governed by the diffusion of H^- ions into the crystal lattice of Co.

The absorption and desorption rates increase with the increase of temperature up to 200 °C. At temperatures higher than 200 °C, the rates decrease with a further increase in temperature (Figs. 3 and 4). At temperatures higher than 200 °C, in the initial stage of absorption, where the overall rate of absorption is controlled by the dissociation of adsorbed hydrogen molecules, a further increase in temperature induces differences between the enthalpy change of adsorbed hydrogen molecules and that of adsorbed hydrogen atoms and H^- ions. Namely, the increase in the enthalpy of H^- ions and H_{ad} species is much more rapid than that of adsorbed hydrogen molecules, $H_{2,ad}$ as induced by temperature. The different enthalpy changes lead to an increase in the activation energy of reaction (2) as illustrated in Fig. 10.

In the case of hydrogen desorption at temperatures higher than 200 °C, the desorption rate decreases with increasing temperature due to the decrease in surface coverage by adsorbed hydrogen atoms.

In the case of slow diffusion, the diffusion flux is proportional to both the diffusion coefficient and the chemical potential gradient of H^- ions. Under these circumstances, all reaction steps 1–3 are in quasi-equilibrium, suggesting that the chemical potentials of all reaction species are equal. However, in the temperature range of 200–230 °C, the diffusion rate is more strongly affected by the diffusion gradient than the diffusion coefficient.

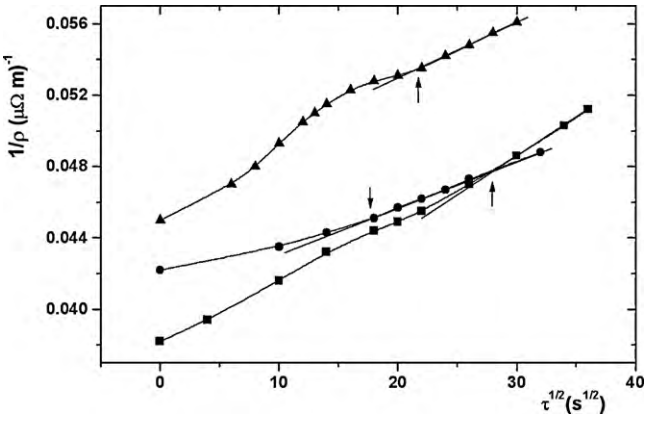

Fig. 9. $1/\rho$ as function of $\tau^{1/2}$ for hydrogen desorption from pressed Co powder at temperatures: (▲) 160 °C; (■) 200 °C; (●) 230 °C.

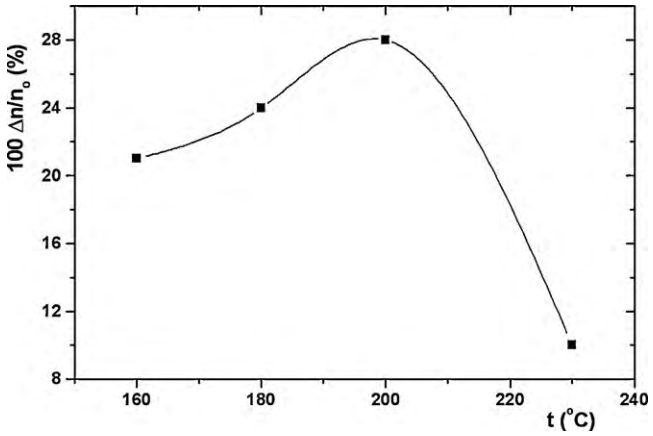

Fig. 11. Calculated values for the relative change in the number of free electrons for the first 150 s of hydrogen absorption on pressed Co powder at various temperatures.

Eq. (10) suggests that hydrogen absorption results in a reduction in the concentration of free electrons in the pressed Co powder. The relative change of the free electron concentration (Fig. 11) is:

$$\frac{\Delta n}{n_0} = 1 - \frac{\rho_0}{\rho} \tag{18}$$

Finally, and most importantly, the experimental results are in agreement with the proposed mechanism of hydrogen absorption/desorption on the pressed Co powder. The adsorbed hydrogen molecules dissociate to adsorbed hydrogen atoms which diffuse into the Co crystal lattice, simultaneously trapping one electron from the conductance band of Co, causing an increase in the electrical resistivity of Co. Conversely, the electrical resistivity decreases during hydrogen desorption.

5. Conclusions

Hydrogen absorption into pressed Co powder causes an increase in its electrical resistivity. The adsorbed hydrogen atoms diffuse into the Co crystal lattice, simultaneously trapping one electron from the conductance band and forming H^- ions, inducing an increase in electrical resistivity. In the initial period of absorption, the dissociation of adsorbed hydrogen molecules is identified as the rate-determining step. After the appropriate concentration of H^- ions in the Co crystal lattice is reached, the reaction becomes controlled by diffusion of H^- ions into bulk cobalt. The initial desorption rate is governed by recombination of adsorbed hydrogen

atoms. For prolonged desorption, the overall reaction rate is controlled by diffusion of H^- ions.

Acknowledgements

The financial support from the Ministry of Science and Technological Development of the Republic of Serbia through Project No. 142 011 G is acknowledged.

References

[1] S. Barrett, Fuel Cells Bull. 2005 (2005) 12–17.
[2] H. Dhaou, F. Askri, M. Ben Salah, A. Jemni, S. Ben Nasrallah, J. Lamloumi, Int. J. Hydrogen Energy 32 (2007) 576–587.
[3] Jing Liu, Xu Zhang, Qian Lia, Kuo-Chin Chou, Kuang-Di Xu, Int. J. Hydrogen Energy 34 (2009) 1951–1957.
[4] S.E. Moradi, S. Amirmahmoodi, M.J. Baniamerian, J. Alloys Compd. 498 (2010) 168–171.
[5] Seong-Hyeon Hong, Sung Nam Kwon, Jong-Soo Bae, Myoung Youp Song, Int. J. Hydrogen Energy 34 (2009) 1944–1950.
[6] I.P. Jain, M.I.S. Abu Dakka, Int. J. Hydrogen Energy 27 (2002) 395–401.
[7] T. Nakagawa, A. Inomata, H. Aoki, T. Miura, Int. J. Hydrogen Energy 24 (1999) 1027–1032.
[8] D. Mat, Y. Kaplan, Int. J. Hydrogen Energy 26 (2001) 957–963.
[9] K. Aldas, D. Mat, Y. Kaplan, Int. J. Hydrogen Energy 27 (2002) 1063–1069.
[10] F. Askri, A. Jemni, S.Ben Nasrallah, Int. J. Hydrogen Energy 28 (2003) 537–557.
[11] F. Askri, A. Jemni, S.Ben Nasrallah, Int. J. Hydrogen Energy 29 (2004) 195–208.
[12] J. Huot, M.L. Tremblay, R. Schulz, J. Alloys Compd. 356 (2003) 603–607.
[13] H. Imamura, M. Kusuhara, S. Minami, M. Matsumoto, K. Masanari, Y. Sakata, Acta Mater. 51 (2003) 6407–6414.
[14] W. Oelerich, T. Klassen, R. Bormann, J. Alloys Compd. 322 (2001) 15–19.
[15] Z. Dehovche, T. Klassen, W. Oelerich, J. Goyette, T.K. Bose, R. Schulz, J. Alloys Compd. 347 (2002) 319–323.
[16] G. Barkhordarian, T. Klassen, R. Bormann, Scripta Mater. 49 (2003) 213–217.
[17] G. Barkhordarian, T. Klassen, R. Bormann, J. Alloys Compd. 407 (2006) 249–255.
[18] N. Hanada, E. Hirotoshi, T. Ichikawa, E. Akiba, H. Fujii, J. Alloys Compd. 450 (2008) 395–399.
[19] Q. Li, Q. Lin, Li. Jiang, K.C. Chou, J. Alloys Compd. 368 (2004) 101–105.
[20] H.Z. Chi, C.P. Chen, L.X. Chen, Q.D. Wang, J. Alloys Compd. 360 (2003) 312–315.
[21] K.J. Gross, D. Chartouni, E. Leroy, A. Ziittel, L. Schlapbach, J. Alloys Compd. 269 (1998) 259–270.
[22] L.H. Gao, C.P. Chen, L.X. Chen, X.H. Wang, J.W. Zhang, X.Z. Xiao, et al., J. Alloys Compd. 399 (2005) 178–182.
[23] X.B. Zhang, D.Z. Sun, W.Y. Yin, Y.J. Chai, M.S. Zhao, Electrochim. Acta 50 (2005) 2911–2918.
[24] B. Liao, Y.Q. Lei, L.X. Chen, G.L. Lu, H.G. Pan, Q.D. Wang, J. Power Sources 129 (2004) 358–367.
[25] Fa-Liang Zhang, Yong-Chung Luo, Jiang-Ping Chen, Ru-Xu Yan, Jian-Hong Chen, J. Alloys Compd. 430 (2007) 302–307.
[26] D.F. Tefer, I.M. Robertson, H.K. Birnbaum, Acta Mater. 49 (2001) 4313–4323.
[27] C.L. Briant, Z.F. Wang, N. Chollocoop, Corros. Sci. 44 (2002) 1875–1888.
[28] A.M. Alvarez a, I.M. Robertson b, H.K. Birnbaum, Acta Mater. 52 (2004) 4161–4175.
[29] E. Tal-Gutelmacher, D. Eliezer, J. Alloys Compd. 404 (2005) 621–625.
[30] Q. Li, L.J. Jiang, K.C. Chou, Q. Lin, F. Zhan, K.D. Xu, X.G. Lu, J.Y. Zhang, J. Alloys Compd. 399 (2005) 101–105.
[31] L. Ming, A.J. Goudy, J. Alloys. Compd. 283 (1999) 146–150.
[32] C.S. Wang, X.H. Wang, Y.Q. Lei, C.P. Chen, Q.D. Wang, J. Hydrogen Energy 21 (1996) 471–478.
[33] M.H. Mintz, Y. Zeiri, J. Alloys Compd. 216 (1994) 159–175.
[34] F. Hua, K. Mon, P. Pasupathi, G.M. Gordon, D.W. Shoesmith, Corrosion, NACE International, Houston, TX, 2004, paper no 04689.
[35] R.W. Schutz, Corrosion 59 (2003) 1043–1057.
[36] Xiaoli Wang, Yongqing Zhao, Yaoqi Wang, Hongliang Hou, Weidong Zeng, J. Alloys Compd. 490 (2010) 562–567.
[37] L. Yan, S. Ramamurthy, J.J. Noël, D.W. Shoesmith, Electrochim. Acta 52 (2006) 1169–1181.
[38] A.F. Denzine, M.S. Reading, Mater. Perf. 37 (1988) 35–41.
[39] P.A. Cella, S.R. Taylor, Corrosion 56 (2000) 951–959.
[40] S. Haruyama, T. Tsuru, Corros. Sci. 13 (1973) 275–285.
[41] T. Tsuru, S. Haruyama, Corros. Sci. 16 (1976) 623–635.
[42] K. Azumi, K. Iokibe, T. Ueno, M. Seo, Corros. Sci. 44 (2002) 1329–1341.
[43] T. Mizuno, M. Enyo, in: R.E. White, B.E. Conwey, J.O'M. Bockris (Eds.), Modern Aspects of Electrochemistry, Vol.30, Plenum Press, New York, 1996, pp. 415–503.
[44] P. Tripodi, N. Armanet, V. Asarisi, A. Avveduto, A. Marmigi, J.D. Vinko, J.P. Biberian, Phys. Lett. A 373 (2009) 3101–3108.
[45] P. Tripodi, N. Armanet, V. Asarisi, A. Avveduto, A. Marmigi, J.P. Biberian, J.D. Vinko, Phys. Lett. A 373 (2009) 4301–4306.
[46] S. Crouch-Baker, M.C.H. McKubre, F.L. Tanzella, J. Phys. Chem. 204 (1998) 247–254.
[47] J. Tóth, L. Péter, I. Bakonyi, K. Tompa, J. Alloys Compd. 387 (2005) 172–178.
[48] P. Tripodi, D. Gioacchino, J.D. Vinko, J. Alloys Compd. 486 (2009) 55–59.
[49] P. Tripodi, A. Avveduto, J.D. Vinko, J. Alloys Compd. 500 (2010) 1–4.
[50] M.M. Antonova, OR: Svoistva Gidridov Metallov: Spravochnik, Naukova Dumka, Kiev, 1975.
[51] K. Gesi, Y. Takagi, J. Phys. Soc. Jpn. 18 (1963) 306–312.
[52] N.E. Paton, B.S. Hickman, D.H. Leslie, Metall. Trans. 2 (1971) 2793–2798.
[53] S.V. Ariyaratnam, N.A. Suplise, E.H. Adem, J. Mater. Sci. Lett. 11 (1987) 1349–1350.
[54] A. Leela Mohana Reddy, G. Srinivas, S. Ramaprabhu, Int. J. Hydrogen Energy 32 (2007) 3356–3362.
[55] M. Singh, Int. J. Hydrogen Energy 21 (1996) 223–228.
[56] B. Baranowski, F.A. Lewis, W.D. McFall, S. Fillipek, T.C. Witherspoon, Proc. R. Soc. A 386 (1983) 309–332.
[57] S.K. Singh, A.K. Singh, K. Ramakrishna, O.N. Srivastava, Int. J. Hydrogen Energy 10 (1985) 523–529.
[58] H. Fuji, V.K. Sinha, F. Pourarian, W.E. Wallace, J. Less Common Metals 85 (1982) 43–48.
[59] R. Ramesh, K.V.S. Rama Rao, J. Appl. Phys. 76 (1994) 3556–3561.
[60] P. Raj, P. Suryanarayana, A. Sathyamoorthy, K. Shashikaala, K.V. Gopalakrishnan, R.M. Iyer, J. Alloys Compd. 179 (1992) 99–109.
[61] S. Enache, W. Lohstroh, R. Grissen, Phys. Rev. B 69 (2004) 115326–115337.
[62] M. Ryazanov, A. Simon, R.K. Kremer, H. Mattausch, Phys. Rev. B 72 (2005) 92408–92411.
[63] V. Paul-Boncour, S.M. ilipek, I. Marchuk, G. André, F. Bourée, G. Wiesinger, A. Percheron-Guégan, J. Phys: Condens. Matter 15 (2003) 4349–4359.
[64] R. Shivakumar, S. Ramaprabhu, K.V.S. Rama Rao, Hydrogen solubility studies in certain Zr–Tb–$(Fe, Co)_3$ compounds. Ph.D. Thesis, Indian Institute of Technology Madras, India, 2000.
[65] W.E. Wallace, S.K. Malik, in: A.F. Andersess, A.J. Maeland (Eds.), Hydrides for Energy Storage, Pergamon Press, Oxford, 1978, p. 33.
[66] V. Azhazha, A. Grib, G. Khadzhay, B. Merisov, A. Pugachov, Int. J. Hydrogen Energy 28 (2003) 415–418.
[67] Yuh Fukai, Saori Yokota, Juńichi Yanagawa, J. Alloys Compd. 407 (2006) 16–24.
[68] J.F. Cannon, J. Phys. Chem. Ref. Data 3 (1974) 781–824.
[69] D.A. Young, Phase Diagrams of the Elements, University of California Press, Berkley, 1976.
[70] I.T. Belash, V.E. Antonov, E.G. Ponyatovsky, Dokl. Akad. Nauk. SSSR 235 (1977) 128–131.
[71] V.E. Antonov, I.T. Belash, V.Yu. Malyshev, E.G. Ponyatovsky, Dokl. Akad. Nauk. SSSR 272 (1983) 1147–1150.
[72] E.G. Ponyatovsky, V.E. Antonov, I.T. Belash, in: A.M. Prokhorov, A.S. Prokhorov (Eds.), Problems in Solid State Physics, Mir, Moscow, 1984, pp. 109–124.
[73] V.E. Antonov, T.E. Antonova, M. Boier, G. Grosse, F.E. Wagner, J. Alloys Compd. 239 (1996) 198–202.